*Thermochimica Acta*, 32 (1979) 241–256

# TITANIUM AND ZIRCONIUM ACID PHOSPHATE DIHYDRATES: THERMAL BEHAVIOUR AND PHASE CHANGES OF THEIR HYDROGEN, SODIUM AND STRONTIUM FORMS

A. LA GINESTRA AND M. A. MASSUCCI

*Laboratorio di Metodologie Avanzate Inorganiche del C.N.R., Via Montorio Romano, 36-00131 Roma (Italy)*

(Received 11 October 1978)

## ABSTRACT

The thermal behaviour of crystalline titanium or zirconium bis(monohydrogen orthophosphate) dihydrate, $Ti(HPO_4)_2 \cdot 2H_2O$ ($\gamma$-titanium phosphate) and $Zr(HPO_4)_2 \cdot 2H_2O$ ($\gamma$-zirconium phosphate) and their sodium- and strontium-exchanged forms have been investigated. TG and DTA curves are given. The X-ray diffraction patterns of the various phases obtained during the thermal treatment (taken with a high-temperature camera) are also reported.

Some interesting similarities are found in the thermal behaviour of the hydrogen forms of $\gamma$-titanium and $\gamma$-zirconium phosphate. Furthermore, the discontinuous decrease in the first *d*-value in their respective X-ray diffraction patterns during the dehydration processes, suggests that these two exchangers possess a layered structure, as do the corresponding $\alpha$-compounds ($Ti(HPO_4)_2 \cdot H_2O$ and $Zr(HPO_4)_2 \cdot H_2O$).

Comparisons are made between $\alpha$- and $\gamma$-compounds, in hydrogen, sodium and strontium form. Although they have an identical chemical composition, the two series of compounds have different structural arrangements which persist over a wide temperature range. Only at high temperatures (800–900 °C) do the $\gamma$-compounds give the same phases as obtained from the $\alpha$-forms.

## INTRODUCTION

As part of a study concerning the preparation of inorganic ion exchangers by hydrothermal treatment[1], we were able to obtain a new crystalline exchanging phase of titanium phosphate, with formula $Ti(HPO_4)_2 \cdot 2H_2O$[2]. We have called this new material $\gamma$-titanium phosphate in analogy with another crystalline inorganic ion-exchanger prepared by Clearfield et al.[3] having the formula $Zr(HPO_4)_2 \cdot 2H_2O$ and called $\gamma$-zirconium phosphate.

The structure of the $\gamma$-phases is still not known (although Clearfield et al[3]. proposed a structure for $\gamma$-zirconium phosphate) because crystals of suitable size for X-ray structure determination have not yet been obtained. However, much experimental evidence, such as the discontinuous change of the first *d*-value in the X-ray powder patterns during the ion-exchange processes[2] or during the intercalation of organic molecules[4] suggests that these compounds also possess a layered structure as do the corresponding $\alpha$-phases $Ti(HPO_4)_2 \cdot H_2O$ and $Zr(HPO_4)_2 \cdot H_2O$. This layered structure probably differs from that of the $\alpha$-phases in the stacking of the layers and/or in the structure of the layers themselves, as has been recently proposed by Alberti et al.[4]. Taking this as an assumption, the interlayer distances for $Ti(HPO_4)_2 \cdot 2H_2O$ and $Zr(HPO_4)_2 \cdot 2H_2O$ can be derived, as for clays[5] and the same $\alpha$-phases[6], from the first *d*-value of their X-ray powder patterns and are 11.55 and 12.2 Å, respectively.

In a previous paper[2] the ion-exchange properties of $Ti(HPO_4)_2 \cdot 2H_2O$ towards sodium and strontium ions were reported and compared with those of $Zr(HPO_4)_2 \cdot 2H_2O$, $Ti(HPO_4)_2 \cdot H_2O$ and $Zr(HPO_4)_2 \cdot H_2O$. Some important similarities were found between the $\gamma$-phases, while appreciable differences could be observed between the $\alpha$- and $\gamma$-compounds.

In this paper the thermal behaviour of the hydrogen, sodium and strontium forms of $\gamma$-titanium phosphate is reported and compared with that of the corresponding $\gamma$-zirconium phosphate compounds. The solid phases occurring at the different temperatures have been characterized by their composition and X-ray powder patterns. To obtain additional information on $\gamma$-phases, comparisons were also made with the thermal behaviour of the hydrogen and ion-exchanged $\alpha$-phases.

## EXPERIMENTAL

### *Chemicals*

All reagents were Merck "pro analysi" except $TiCl_4$ which was an Erba RP product.

### *Preparation of materials*

(1) $Ti(HPO_4)_2 \cdot 2H_2O$ or $\gamma\text{-TiP}\overline{H_2} \cdot 2H_2O$*: 5 g of amorphous titanium phosphate or the same amount of crystalline monohydrated form $Ti(HPO_4)_2 \cdot H_2O$ ($\alpha\text{-TiP}\overline{H_2} \cdot H_2O$)[7] were sealed in a pyrex tube with 10 M $H_3PO_4$ (70% filling) and hydrothermally treated at 300°C for 24 h. After cooling, the material was filtered, washed with distilled water to pH = 4 and air conditioned.

(2) $\gamma\text{-TiP}\overline{H_{1.5}Na_{0.5}} \cdot H_2O$ was obtained by simply contacting $\gamma\text{-TiP}\overline{H_2} \cdot 2H_2O$ with 0.1 N NaCl solution.

(3) $\gamma\text{-TiP}\overline{HNa} \cdot 3H_2O$ and $\gamma\text{-TiP}\overline{Na_2} \cdot 2H_2O$ were prepared by contacting $\gamma\text{-TiP}\overline{H_2} \cdot 2H_2O$ with a fixed volume of 0.1 N (NaCl + NaOH) solution with NaOH in the appropriate amounts for half and full conversion of the exchanger in sodium ion[2].

---

[*] The different phases will be hereafter indicated with a Greek letter followed by the symbol of the exchanger, their counterions under a bar and water (if present) composition.

(4) $\gamma\text{-Ti}\overline{\text{PHSr}_{0.5}} \cdot 3H_2O$ was prepared in the same way as $\gamma\text{-Ti}\overline{\text{PHNa}} \cdot 3H_2O$ by employing 0.1 N ($SrCl_2 + Sr(OH)_2$) solution[2].

(5) $\gamma\text{-Zr}\overline{\text{PH}_2} \cdot 2H_2O$ was prepared according to Clearfield et al.[3].

(6) $\gamma\text{-Zr}\overline{\text{PHNa}} \cdot 2.5H_2O$, $\gamma\text{-Zr}\overline{\text{PNa}_2} \cdot 3H_2O$ and $\gamma\text{-Zr}\overline{\text{PHSr}_{0.5}} \cdot 3H_2O$ were prepared in the same way as the corresponding $\gamma$-TiP forms[2].

*Apparatus and procedures*

DTA curves were obtained by means of a Gebr. Netzsch 404 apparatus equipped with Pt/10%Pt–Rh thermocouples and platinum containers using a heating rate of 5°C $\text{min}^{-1}$.

TG measurements were performed on a Stanton, Model TG 750, thermobalance. Samples were heated in platinum crucibles in air atmosphere and the heating rate ranged from 1 to 5°C $\text{min}^{-1}$.

X-Ray powder spectra were taken on a Philips diffractometer (Ni filtered Cu $K_\alpha$ radiation). An Italstructure Model AF 3 high-temperature attachment was used when reversible processes, such as the rehydration of some materials or reversible phase transitions, could take place. The heating system consisted of an induction furnace with hemispherical graphite elements. The sample was held on a platinum support, in contact with Pt/10%Pt–Rh thermocouples. The temperatures at which the powder spectra were taken were chosen in correspondence with the inflection points and at the end of each definite weight loss in the TG curves or before and after a thermal effect in the DTA curves.

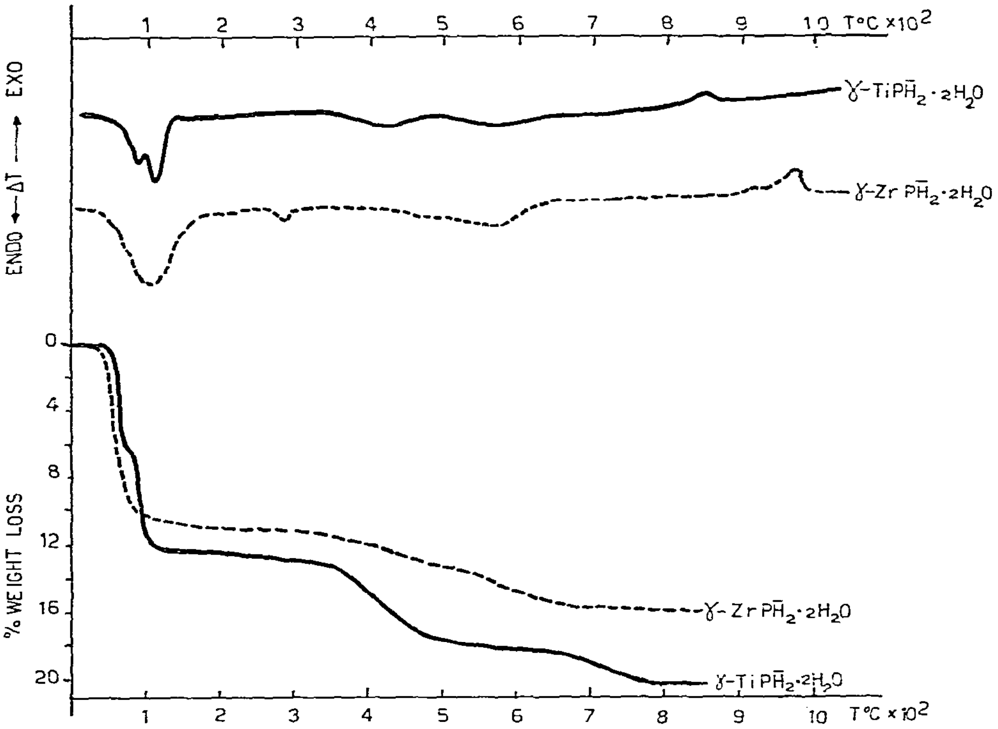

Fig. 1. DTA and TG curves of $\gamma$-$Ti(HPO_4)_2 \cdot 2H_2O$ and $\gamma$-$Zr(HPO_4)_2 \cdot 2H_2O$.

TABLE 1

X-RAY DIFFRACTION PATTERNS OF $\gamma$-Ti$(HPO_4)_2 \cdot 2H_2O$ AND ITS DERIVATIVES AT VARIOUS TEMPERATURES

| $\gamma$-TiP$\overline{H}_2 \cdot 2H_2O$ at 25 °C | $\gamma$-TiP$\overline{H}_2 \cdot H_2O$ at 60 °C | $\gamma$-TiP$\overline{H}_2$ at 120–300 °C | $\gamma$-TiP$\overline{H}_2$ | |
|---|---|---|---|---|
| | | | at 500 °C | at 800 °C ($\alpha$-Ti$P_2O_7$) |
| 11.55 vs | 11.47 s | | | |
| | | 9.20 ms | 8.26 mw | |
| 5.56 mw | 5.48 mw | 5.21 m | | |
| 4.29 mw | | 4.48 vw | | 4.51 m |
| 3.86 w | 3.85 mw | | | 3.91 vs |
| | 3.79 ms | | 3.71 s | |
| | 3.66 vw | | 3.65 m | |
| 3.46 ms | | 3.42 s | | 3.50 s |
| 3.30 w | 3.28 vw | | | |
| 3.17 w | 3.13 w | 3.13 w | | 3.19 s |
| 3.05 w | 3.05 vw | | | |
| | 2.89 w | 2.99 vw | | |
| 2.78 w | | 2.75 vw | | |
| 2.58 vw | | | | |
| 2.55 w | | | | |
| | | 2.41 vw | | |
| | | 2.29 w | | |

vs = very strong; s = strong; m = medium; w = weak; vw = very weak.

## RESULTS AND DISCUSSION

### *Thermal behaviour of the $\gamma$-TiP forms*

*$\gamma$-TiP$\overline{H}_2 \cdot 2H_2O$ (11.55 Å).* From the TG and DTA curves reported in Fig. 1, it can be seen that the 2 moles of hydration water are lost in the range 40–100 °C in two steps (1 mole for each step). The subsequent endothermic reaction is connected to the condensation of the hydrogen phosphate groups to pyrophosphate with the loss of 1 mole of water per mole of exchanger, which occurs in two steps, the first between 350–500 °C, the second between 500–700 °C; $\alpha$-Ti$P_2O_7$ [8] is formed in the latter range.

In Table 1 are reported the X-ray diffraction patterns of $\gamma$-TiP$\overline{H}_2 \cdot 2H_2O$ at room temperature, $\gamma$-TiP$\overline{H}_2 \cdot H_2O$ at 60 °C, $\gamma$-TiP$\overline{H}_2$ at 120 °C (similar to that recorded at 300 °C), an unknown phosphate–pyrophosphate phase obtained at 500 °C and, finally, the spectrum of the sample heated at 800 °C, which corresponds to that of $\alpha$-Ti$P_2O_7$.

We have observed that both $\gamma$-TiP$\overline{H}_2 \cdot H_2O$ (11.47 Å) and $\gamma$-TiP$\overline{H}_2$ (9.2 Å) show a tendency to rehydrate to the dihydrate form when left in air. Furthermore, the two steps observed in the condensation of the hydrogen phosphate groups can be explained by the formation at 500 °C of the unknown phosphate–pyrophosphate phase having first $d$ = 8.3 Å; the decrease of the interlayer distance from 9.2 to 8.3 Å can also account for the slowing down in the second step of the condensation process.

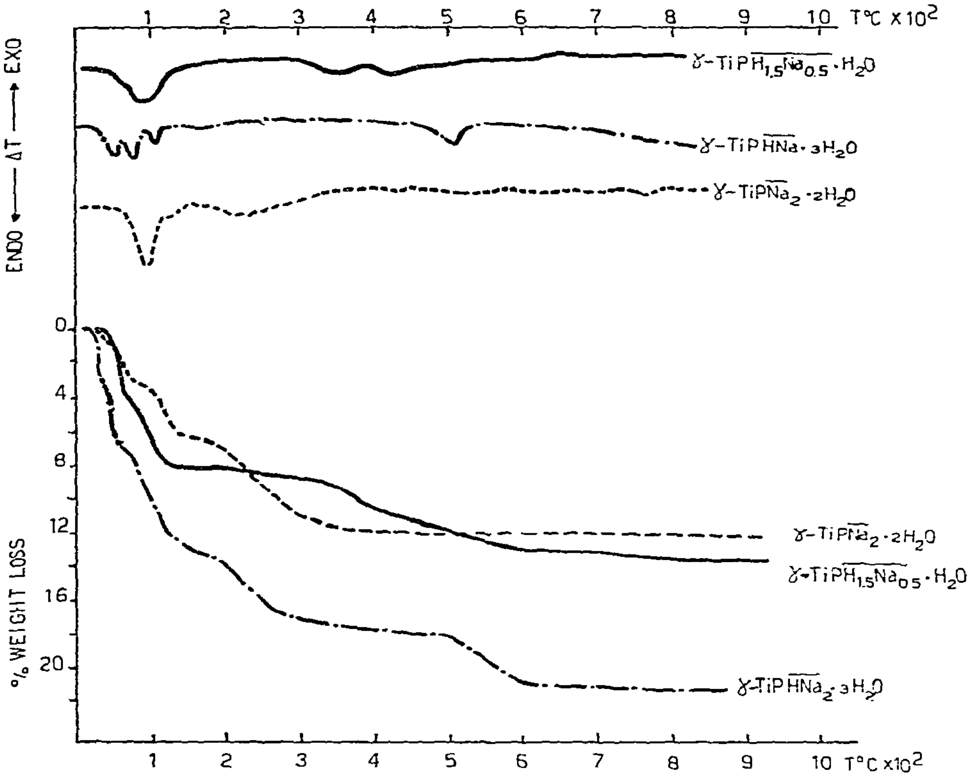

Fig. 2. DTA and TG curves of Na forms of γ-titanium phosphate.

The thermal process can be summarized as follows*

$$\underset{(11.55\ \text{Å})}{\gamma\text{-TiP}\overline{H_2}\cdot 2H_2O} \underset{40\text{–}60\,^\circ\text{C}}{\overset{-H_2O}{\rightleftharpoons}} \underset{(11.47\ \text{Å})}{\gamma\text{-TiP}\overline{H_2}\cdot H_2O} \underset{70\text{–}100\,^\circ\text{C}}{\overset{-H_2O}{\rightleftharpoons}} \underset{(9.2\ \text{Å})}{\gamma\text{-TiP}\overline{H_2}} \xrightarrow[360\text{–}500\,^\circ\text{C}]{-xH_2O}$$

$$\underset{(8.3\ \text{Å})}{\gamma\text{-Ti}(HPO_4)_{2-2x}(P_2O_7)_x} \xrightarrow[550\text{–}700\,^\circ\text{C}]{-(1-x)H_2O} \alpha\text{-TiP}_2O_7$$

$TiP\overline{H_{1.5}Na_{0.5}} \cdot H_2O$ *(11.0 Å)*. DTA and TG curves are reported in Fig. 2 and X-ray spectra in Fig. 3a.

The dehydration process begins at 40 °C and takes place in two steps: about half a mole of water is lost between 40–60 °C and the remainder between 60–120 °C, with a slowing down of the process. The X-ray spectra of the material taken in the high-temperature camera in the range 40–120 °C, show that at 60 °C the monohydrated phase with the interlayer spacing of 11.0 A is no longer present and three new phases are formed with interlayer spacings of 10.8, 10.1 and 9.2 Å, respectively. Since the monohydrated phase should still be present at 60 °C, we suggest that this phase

---

* The numbers in parentheses refer to the interlayer spacing for the compounds that presumably possess a layered structure.

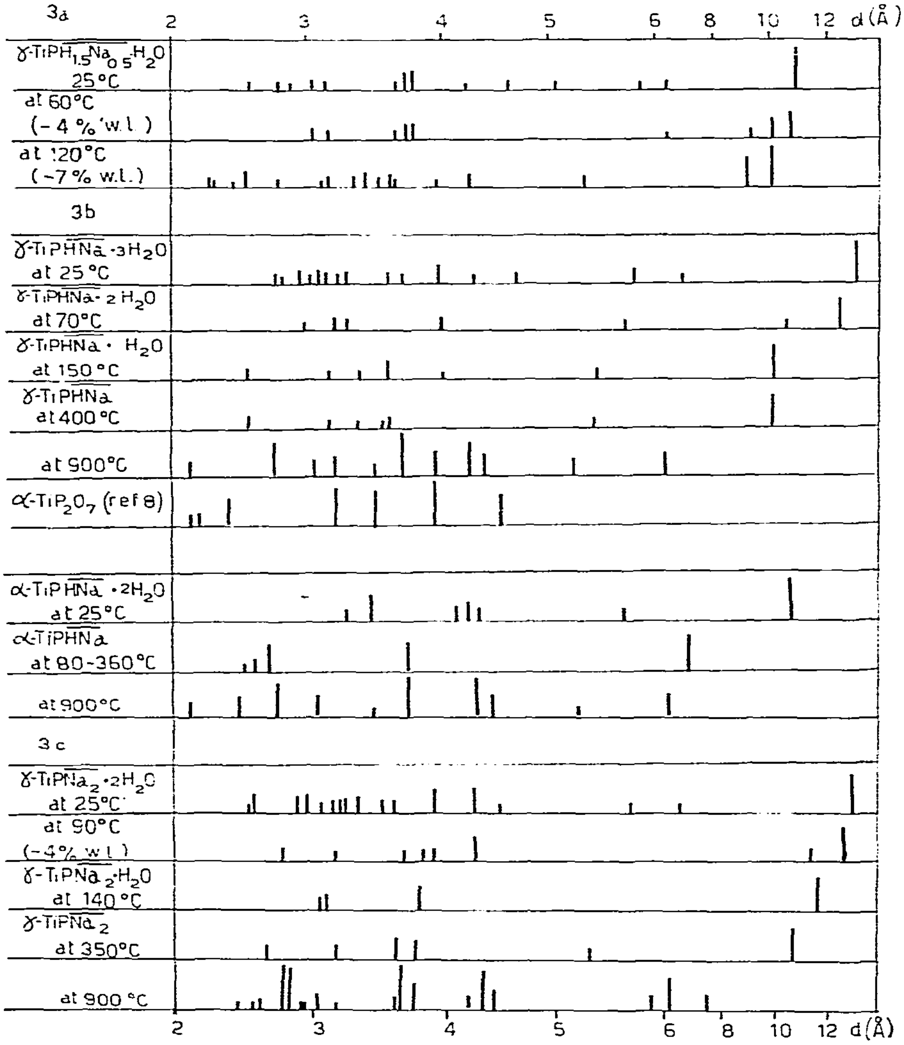

Fig. 3. X-Ray diffraction patterns of Na forms of $\gamma$-titanium phosphate and their derivatives at various temperatures.

transforms into one with a shorter interlayer distance ($d = 10.8$ Å), which may partly be responsible for the slowing down of the dehydration process. At 120°C, when the mole of hydration water is completely lost, only two phases are present (see X-ray spectrum in Fig. 3a), the $\gamma$-Ti$\overline{\mathrm{PH}_2}$ (9.2 Å) and $\gamma$-Ti$\overline{\mathrm{PHNa}}$ (10.1 Å). This means that the anhydrous $\gamma$-TiP$\overline{\mathrm{H}_{1.5}\mathrm{Na}_{0.5}}$ phase is not stable and in its place, the hydrogen and monohydrogen–monosodium anhydrous phases are formed. These phases subsequently follow their own thermal behaviour, the former as we have seen before, the latter as will be discussed below.

The thermal process (omitting their stoichiometry when several phases are present together) is

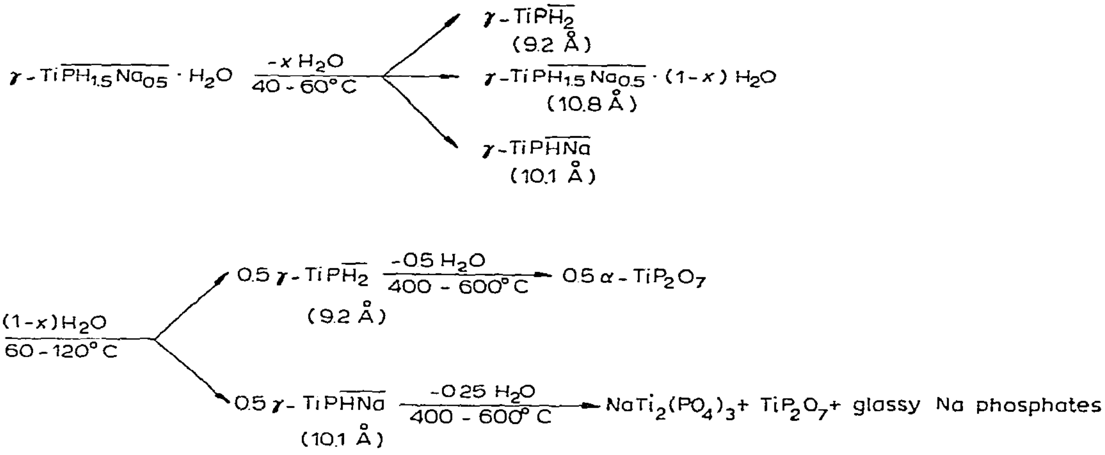

*γ-Ti$\overline{PHNa}$ · 3H$_2$O* (13.2 *Å*). TG and DTA curves are reported in Fig. 2 and X-ray patterns in Fig. 3b.

The first mole of water is lost in two steps in the range 30–70 °C, the second 70–150 °C, and the third 150–400 °C, each in a single step. The dihydrated phase with $d = 12.6$ Å, begins to form at about 30 °C and ends at 70 °C, but at this temperature the monohydrated phase is also formed and its first reflection is at 10.65 Å (see spectrum, Fig. 3b). On increasing the temperature, the intensities of the monohydrated phase reflections become stronger but at the same time its first reflection shifts gradually from 10.65 to 10.2 Å. The monohydrated and anhydrous phases have very similar interlayer spacings and a comparison of their other reflections seems to indicate that their structures are not very different (see spectra at 150 and 400 °C). At 500 °C the condensation of the hydrogenphosphate groups begins and at a temperature > 700 °C we can observe the reflections of the $\alpha$-TiP$_2$O$_7$ and those of the sodium dititanium triphosphate[15], the latter being similar to those of the phase obtained from $\alpha$-Ti$\overline{PHNa}$ (Fig. 3b). The formation of NaTi$_2$(PO$_4$)$_3$ phase must be accompanied by the formation of sodium phosphates, undetectable in the X-ray diffraction patterns because of their glassy nature. The process can be summarized

$$\underset{(13.2\ \text{Å})}{\gamma\text{-Ti}\overline{\text{PHNa}}\cdot 3\text{H}_2\text{O}} \xrightarrow[30-70^\circ\text{C}]{-\text{H}_2\text{O}} \underset{(12.6\ \text{Å})}{\gamma\text{-Ti}\overline{\text{PHNa}}\cdot 2\text{H}_2\text{O}} \xrightarrow[70-150^\circ\text{C}]{-\text{H}_2\text{O}} \underset{(10.2\ \text{Å})}{\gamma\text{-Ti}\overline{\text{PHNa}}\cdot \text{H}_2\text{O}}$$

$$\xrightarrow[150-400^\circ\text{C}]{-\text{H}_2\text{O}} \underset{(10.1\ \text{Å})}{\gamma\text{-Ti}\overline{\text{PHNa}}} \xrightarrow[500-700^\circ\text{C}]{-0.5\ \text{H}_2\text{O}} \text{NaTi}_2(\text{PO}_4)_3 + \alpha\text{-TiP}_2\text{O}_7 + \text{glassy Na phosphates}$$

*γ-Ti$\overline{PNa_2}$ · 2H$_2$O* (12.8 *Å*). The TG and DTA curves are reported in Fig. 2 and the X-ray patterns in Fig. 3c.

The first mole of water is lost in two steps. The X-ray spectrum of the material taken at 90°C at the inflection point in the TG curve (4% weight loss), shows the presence of two phases: $\gamma$-$\overline{\mathrm{TiPNa_2}}\cdot 2H_2O$, with the interlayer distance shortened to 12.65 Å (responsible for the slowing down of this dehydration process), and $\gamma$-$TiPNa_2 \cdot H_2O$ with an interlayer distance of 11.5 Å. The last molecule of water is lost in the range 150–350°C with the formation of the anhydrous phase ($d$ = 10.6 Å). At higher temperatures, the reflections of $NaTi_2(PO_4)_3$ are observed with others which must be due to a gradually disappearing layered phase (7.24 Å). The DTA curve does not show the presence of a clear thermal effect connected with the involved processes.

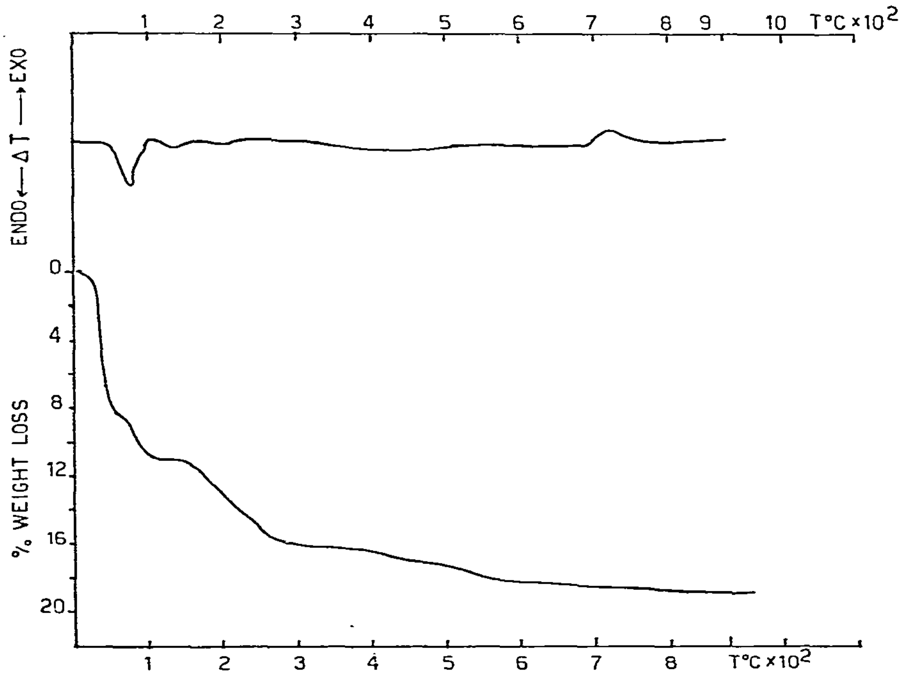

Fig. 4. DTA and TG curves of $\gamma$-$TiHSr_{0.5}(PO_4)_2 \cdot 3H_2O$.

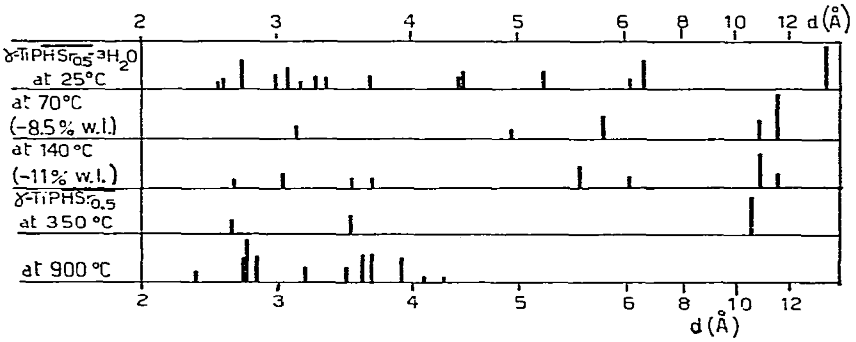

Fig. 5. X-Ray diffraction patterns of $\gamma$-$TiHSr_{0.5}(PO_4)_2 \cdot 3H_2O$ and its derivatives at various temperatures.

The process can be summarized

$$\underset{(12.8\ \text{Å})}{\gamma\text{-TiP}\overline{Na_2}\cdot 2H_2O} \xrightarrow[50\text{–}140\,^\circ C]{-H_2O} \underset{(11.5\ \text{Å})}{\gamma\text{-TiP}\overline{Na_2}\cdot H_2O} \xrightarrow[160\text{–}350\,^\circ C]{-H_2O}$$

$$\underset{(10.6\ \text{Å})}{\gamma\text{-TiP}\overline{Na_2}} \xrightarrow[500\text{–}800\,^\circ C]{} \underset{(7.24\ \text{Å})}{[TiNa_2(PO_4)_2]} + NaTi_2(PO_4)_3 + \text{glassy Na phosphates}$$

*$\gamma$-TiP$\overline{HSr_{0.5}}\cdot 3H_2O$ (13.4 Å).* The TG and DTA curves are reported in Fig. 4 and X-ray patterns in Fig. 5. The first two molecules of crystal water are lost below 140 °C in two steps and the third in the range 150–350 °C. In correspondence with the first inflection point of the TG curve (60–70 °C), when about 1.5 moles of hydration water are lost, the X-ray pattern shows the presence of two phases with 11.6 and 10.95 Å as a first *d*-value, respectively. We suggest that the initial trihydrate phase changes into a dihydrate having a shorter interlayer distance (11.6 Å), the other phase is $\gamma$-TiP$\overline{HSr_{0.5}}\cdot H_2O$ (10.95 Å). The endothermal reaction due to the condensation process is poorly evident in the DTA curve because of the wide temperature range in which it occurs. At about 700 °C the exothermic reaction is probably due to the crystallization of a compound not known in the literature which could be a double phosphate of Sr and Ti, as double phosphates are obtained when similar compounds of the zirconium phosphate exchanged with divalent ions (Ca, Mn, Co, Ni, Cu and Zn) are heated above 700 °C[9, 10]. At 900 °C reflections of $\alpha$-TiP$_2$O$_7$ are also observed (see Figs. 5a and 3b).

Summarizing, the process is

$$\underset{(13.4\ \text{Å})}{\gamma\text{-TiP}\overline{HSr_{05}}\cdot 3H_2O} \xrightarrow[40-140^\circ C]{-2H_2O} \underset{(1095\ \text{Å})}{\gamma\text{-TiP}\overline{HSr_{05}}\cdot H_2O} \xrightarrow[140-350^\circ C]{-H_2O}$$

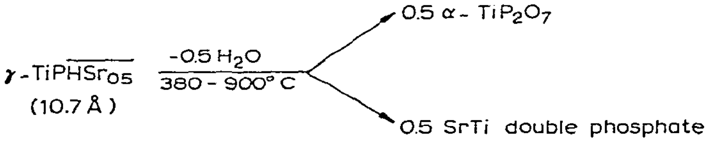

At this point it was interesting to make a comparison between the $\gamma$- and $\alpha$-forms of TiP. The pairs of compounds to be compared are $\gamma$- and $\alpha$-TiP$\overline{H_2}\cdot H_2O$ and $\gamma$- and $\alpha$-TiP$\overline{HNa}\cdot 2H_2O$, and their respective anhydrous $\gamma$- and $\alpha$-forms. From the X-ray diffraction patterns it can be noted that no similarities are found among these pairs of compounds. The $\gamma$-compounds always have an interlayer spacing higher than the corresponding $\alpha$-forms. Besides, the DTA and TG curves show that the condensation process occurs at different temperatures for the components of the two pairs of anhydrous phases considered. Only when heated at high temperatures (~850–900 °C) do the samples give the same TiP$_2$O$_7$ or, for the $\overline{HNa}$-forms, the same sodium dititanium triphosphate.

The different thermal behaviour of $\gamma$- and $\alpha$-compounds can be ascribed to a different starting structural arrangement of these two series of exchangers.

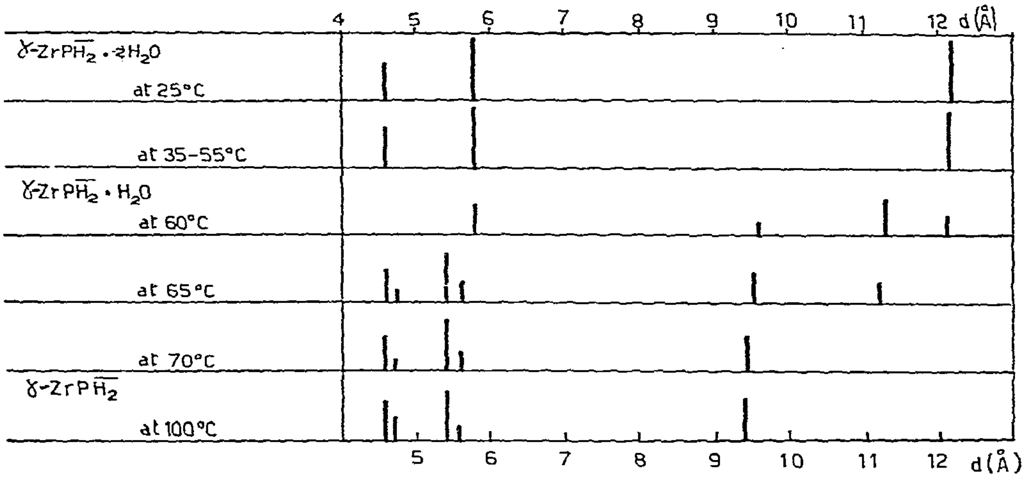

Fig. 6. X-Ray diffraction patterns of $\gamma$-Zr(HPO$_4$)$_2$ · 2H$_2$O in the range 25–100°C recorded with a high-temperature camera.

TABLE 2

X-RAY DIFFRACTION PATTERNS OF $\gamma$-Zr(HPO$_4$)$_2$ · 2H$_2$O AND ITS DERIVATIVES AT VARIOUS TEMPERATURES

| *$\gamma$-ZrP$\overline{H}_2$ · 2H$_2$O at 25°C* | *$\gamma$-ZrP$\overline{H}_2$ at 100–250°C* | *$\gamma$-ZrP$\overline{H}_2$ at 300–350°C* | *$\gamma$-ZrP$\overline{H}_2$* | |
|---|---|---|---|---|
| | | | *at 550°C* | *at 900°C ($\alpha$-ZrP$_2$O$_7$)* |
| 12.20 s | | | | |
| | 9.45 mw | 9.45 w | 8.3 vw | |
| 5.80 vs | | | | |
| | 5.40 s | 5.39 m | | |
| | | 5.19 mw | 5.16 m | |
| 4.60 m | 4.70 mw | 4.72 mw | | 4.77 m |
| | 4.62 m | 4.58 m | | |
| 4.48 m | | | | |
| 4.35 m | 4.39 vvw | 4.39 vvw | | |
| | 4.11 vvw | 4.13 vvw | | 4.13 vs |
| 3.74 mw | 3.82 w | 3.82 mw | 3.86 vs | |
| | 3.57 ms | 3.57 ms | | 3.69 m |
| | 3.51 m | | | |
| 3.31 s | 3.30 vs | 3.29 vs | 3.30 s | 3.38 mw |
| 3.19 m | 3.16 w | 3.17 w | | |
| | 3.11 w | 3.12 w | 3.10 vvw | |
| | 2.88 vvw | 2.89 vvw | | 2.91 m |
| 2.68 m | 2.69 mw | 2.68 m | 2.69 mw | 2.76 w |
| | 2.55 vvw | 2.54 vvw | 2.59 mw | |
| | 2.49 vvw | | 2.51 mw | 2.49 m |
| | 2.43 vvw | 2.42 vvw | | 2.39 w |
| 2.17 w | | 2.14 vvw | 2.13 w | |
| | | | 2.03 vvw | |
| | | | 1.93 vw | |

vs = very strong; s = strong; m = medium; w = weak; vw = very weak.

*Thermal behaviour of γ-ZrP forms*

$\gamma\text{-}ZP\overline{H}_2 \cdot 2H_2O$ (12.2 *Å*). The thermal behaviour has already been studied by Dollimore et al.[11]. Our data allow us to identify the structural variations connected with the various processes occurring during the thermal treatment. DTA and TG curves (Fig. 1) seem to show that the two molecules of water are eliminated in a single step between 35 and 120 °C. However, carrying TG experiments at a very slow heating rate we have observed a slight inflection at about 60 °C corresponding to the loss of 1 mole of water. In Fig. 6 is reported the sequence of the X-ray powder spectra between 20 and 100 °C obtained with a high-temperature apparatus. It can be seen that at 60–65 °C, when the reflection at 12.2 Å disappears, two new reflections at 11.3 and 9.6 Å (the latter going to 9.45 Å with increase in the temperature) are observed. At 70 °C only the 9.45 Å reflection is present. The sequence provides clear evidence that $\gamma\text{-ZP}\overline{\text{H}}_2 \cdot 2\text{H}_2\text{O}$ dehydrates in two steps, but the monohydrated phase, with an interlayer distance of 11.3 Å, is not easily separable from the anhydrous phase (9.45 Å) because of the very narrow temperature range in which it can exist. Both the dehydration processes are reversible.

Between 80 and 250 °C the powder spectrum of the anhydrous phase does not show any change (Table 2). Between 250 and 350 °C an endothermal (see DTA curve) and reversible phase change is observed. Notwithstanding this, the X-ray spectrum of the material is very similar to that at 250 °C, as if only slight structural modifications had taken place. In fact, the interlayer distance is about the same and only small differences are found in the intensities and the *d*-values of the other

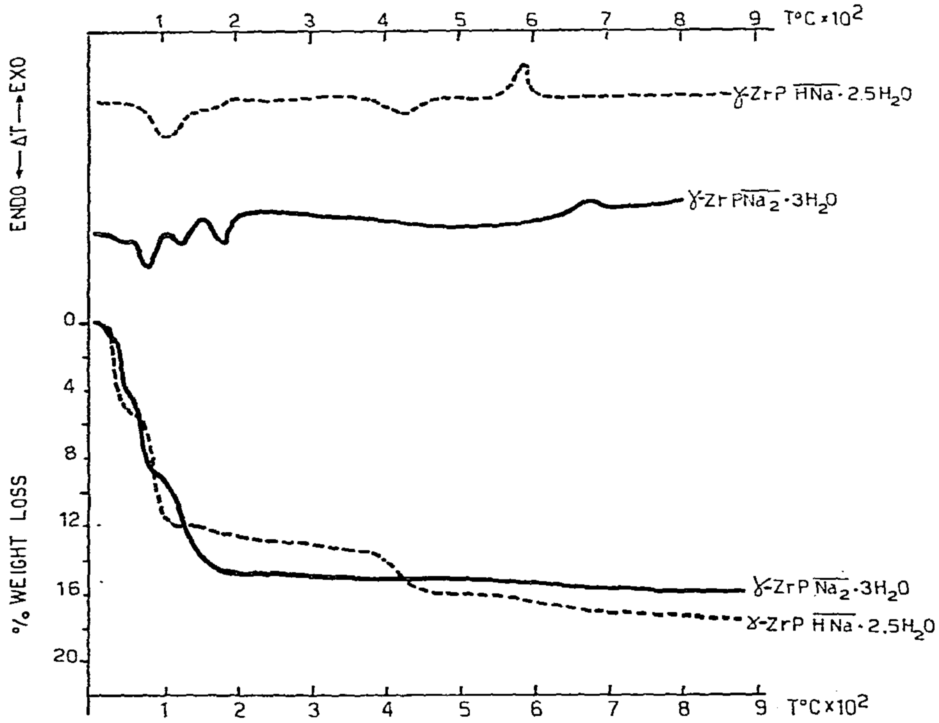

Fig. 7. DTA and TG curves of Na forms of γ-zirconium phosphate.

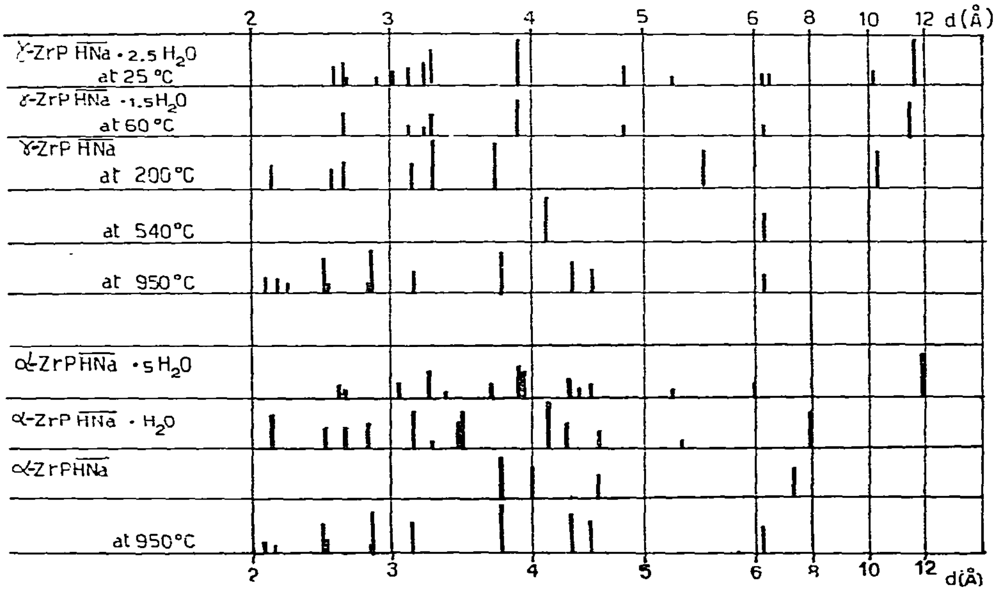

Fig. 8. X-Ray diffraction patterns of monohydrogen-monosodium-forms of $\gamma$- and $\alpha$-zirconium phosphates and their derivatives at various temperatures.

reflections. By way of contrast, in the case of anhydrous $\alpha\text{-ZrP}\overline{\text{H}_2}$ and $\alpha\text{-TiP}\overline{\text{H}_2}$, the analogous reversible endothermal effect, occurring at about 200°C and 290°C, respectively, provokes a drastic change in the structure of these materials[12].

The condensation process begins at 360°C. The observed slowing down between 500 and 700°C should be due to the formation of a phase with an interlayer distance of 8.3 Å (as observed during the condensation of the $\gamma\text{-TiP}\overline{\text{H}_2}$ phase) rather than to the formation of an intermediate type $Zr_3(HPO_4)_2\ (P_2O_7)_2$[11], in correspondence with the inflection point in the TG curve, since the weight loss corresponding to the intermediate is not always the same but depends on the rate of temperature increase.

At 900°C $\alpha\text{-ZrP}_2\text{O}_7$[13] is formed after the slight exothermic reaction at 870°C, which is the minimum temperature at which $\gamma$- and $\alpha$-zirconium phosphate give rise to the same phase.

The process can be written as follows

$$\underset{(12.2\,\text{Å})}{\gamma\text{-ZrP}\overline{\text{H}_2}\cdot 2H_2O} \underset{30\text{–}65\,°\text{C}}{\overset{-H_2O}{\rightleftharpoons}} \underset{(11.3\,\text{Å})}{\gamma\text{-ZrP}\overline{\text{H}_2}\cdot H_2O} \underset{65\text{–}80\,°\text{C}}{\overset{-H_2O}{\rightleftharpoons}} \underset{(9.5\,\text{Å})}{\gamma\text{-ZrP}\overline{\text{H}_2}}$$

$$\underset{270\text{–}290\,°\text{C}}{\overset{\text{rev. phase transition}}{\rightleftharpoons}} \underset{(9.5\,\text{Å})}{\gamma\text{-ZrP}\overline{\text{H}_2}} \xrightarrow[370\text{–}500\,°\text{C}]{-xH_2O} \underset{(8.3\,\text{Å})}{\gamma\text{-Zr(HPO}_4)_{2-2x}(\text{P}_2\text{O}_7)_x}$$

$$\xrightarrow[500\text{–}700\,°\text{C}]{-(1-x)H_2O} \underset{(8.3\,\text{Å})}{\gamma\text{-ZrP}_2\text{O}_7} \xrightarrow[870\text{–}980\,°\text{C}]{\text{phase transition}} \alpha\text{-ZrP}_2\text{O}_7$$

*$\gamma\text{-ZrP}\overline{\text{HNa}}\cdot 2.5H_2O$ (11.6 Å).* Taking into account the DTA and TG curves (Fig. 7) and the X-ray patterns (Fig. 8) taken in correspondence with the inflection

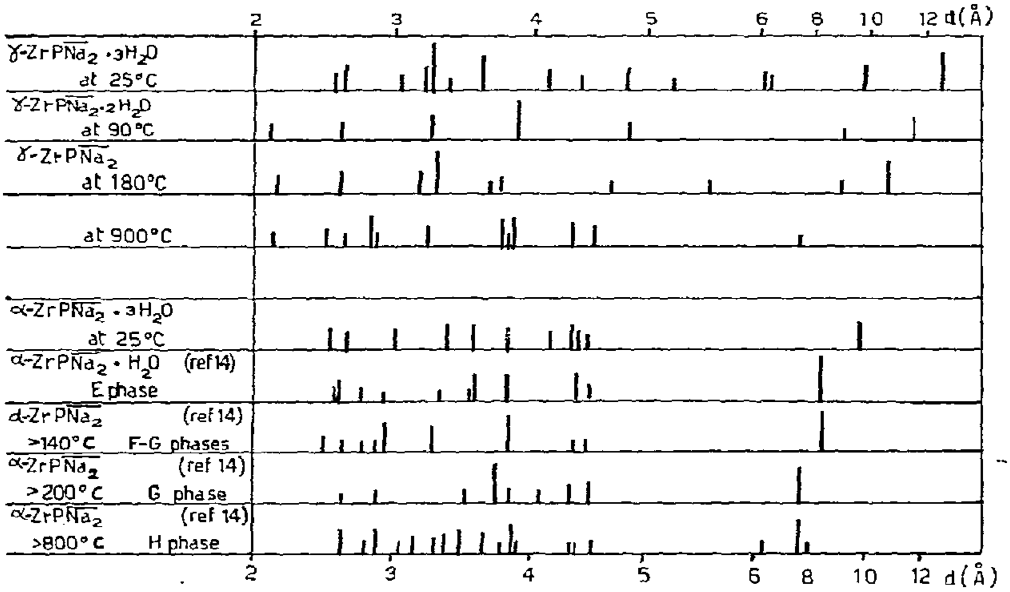

Fig. 9. X-Ray diffraction patterns of disodium forms of $\gamma$- and $\alpha$-zirconium phosphates and their derivatives at various temperatures.

points of the TG curves and particular points on DTA, the thermal process can be summarized

$$\underset{(11.6\ \text{Å})}{\gamma\text{-Zr}\overline{\text{PHNa}}\cdot 2.5H_2O} \xrightarrow[40\text{–}60\,^{\circ}\text{C}]{-H_2O} \underset{(11.5\ \text{Å})}{\gamma\text{-Zr}\overline{\text{PHNa}}\cdot 1.5H_2O} \xrightarrow[60\text{–}200\,^{\circ}\text{C}]{-1.5H_2O}$$

$$\underset{(10.3\ \text{Å})}{\gamma\text{-Zr}\overline{\text{PHNa}}} \xrightarrow[380\text{–}430\,^{\circ}\text{C}]{-0.5H_2O} \underset{(6.2\ \text{Å})}{\gamma\text{-Zr}_2\text{Na}_2(\text{PO}_4)_2\ \text{P}_2\text{O}_7}$$

$$\xrightarrow[560\text{–}650\,^{\circ}\text{C}]{\text{phase transition}} \text{NaZr}_2(\text{PO}_4)_3 + \text{glassy Na phosphates}$$

Only after the exothermic peak at 560–600 °C is the phase obtained from $\gamma$-Zr$\overline{\text{PHNa}}$ similar to that of $\alpha$-Zr$\overline{\text{PHNa}}$ heated at the same temperature (see Fig. 8). It is evident that this exothermic reaction is connected to the formation of the $\text{NaZr}_2(\text{PO}_4)_3$.

*$\gamma$-Zr$\overline{PNa_2}$ · $3H_2O$ (12.6 Å).* This compound eliminates the 3 moles of water below 200 °C in three steps, each corresponding to 1 mole of water. The interlayer distance correspondingly decreases, but is always higher than the corresponding first *d*-value of the $\alpha$-phases at the same hydration degree (Fig. 9).

In the range 650–750 °C a broad exothermic peak, connected with a phase change, is evident in the DTA curve and leads to the formation of the $\text{NaZr}_2(\text{PO}_4)_3$ phase[15]. The X-ray patterns at 900 °C show that a layered phase at 7.43 Å is still present in a small amount, as observed in the case of $\gamma$-Ti$\overline{\text{PNa}_2}$ at the same temperature. A multiphase system seems to be present also in the case of $\alpha$-Zr$\overline{\text{PNa}_2}$ in the

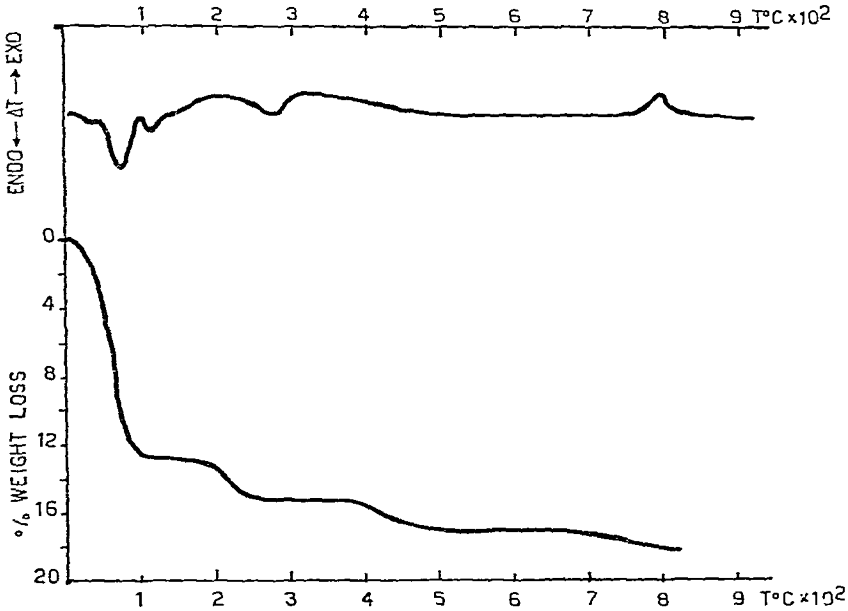

Fig. 10. DTA and TG curves of $\gamma$-ZrHSr$_{0.5}$(PO$_4$)$_2$ · 3H$_2$O.

same temperature range, as suggested by the X-ray spectrum of the phase indicated by Clearfield and Medina as phase H[14].

The thermal process is

$$\underset{(12.6\ \text{Å})}{\gamma\text{-Zr}\overline{\text{PNa}_2}\cdot 3\text{H}_2\text{O}} \xrightarrow[40\text{–}90\,^\circ\text{C}]{-2\text{H}_2\text{O}} \underset{(11.6\ \text{Å})}{\gamma\text{-Zr}\overline{\text{PNa}_2}\cdot \text{H}_2\text{O}} \xrightarrow[90\text{–}180\,^\circ\text{C}]{-\text{H}_2\text{O}}$$

$$\underset{(10.7\ \text{Å})}{\gamma\text{-Zr}\overline{\text{PNa}_2}} \xrightarrow[650\text{–}750\,^\circ\text{C}]{\text{exothermic reaction}} \text{NaZr}_2(\text{PO}_4)_3 + \underset{(7.43\ \text{Å})}{[\text{ZrNa}_2(\text{PO}_4)_2]} + \text{glassy Na phosphates}$$

*$\gamma$-Zr$\overline{\text{PHSr}_{0.5}}\cdot 3H_2O$ (12.8 Å).* TG and DTA curves are reported in Fig. 10 and X-ray patterns in Fig. 11. Taking into account the weight loss and the phase transition, the process can be schematized as follows

$$\underset{(12.8\ \text{Å})}{\gamma\text{-Zr}\overline{\text{PHSr}_{0.5}}\cdot 3\text{H}_2\text{O}} \xrightarrow[40\text{–}120\,^\circ\text{C}]{-2.5\text{H}_2\text{O}} \underset{(11.3\ \text{Å})}{\gamma\text{-Zr}\overline{\text{PHSr}_{0.5}}\cdot 0.5\text{H}_2\text{O}} \xrightarrow[180\text{–}260\,^\circ\text{C}]{-0.5\text{H}_2\text{O}}$$

$$\underset{(11.2\ \text{Å})}{\gamma\text{-Zr}\overline{\text{PHSr}_{0.5}}} \xrightarrow[380\text{–}550\,^\circ\text{C}]{-0.5\text{H}_2\text{O}} \underset{\text{(low temperature phase)}}{\text{ZrSr}(\text{PO}_4)_2\text{P}_2\text{O}_7}$$

$$\xrightarrow[750\text{–}830\,^\circ\text{C}]{\text{phase transition}} \underset{\text{(high temperature phase)}}{\text{ZrSr}(\text{PO}_4)_2\text{P}_2\text{O}_7}$$

From the X-ray diffraction patterns (Table 2 and Figs. 8, 9 and 11) the comparison between the hydrogen, hydrogen-sodium, sodium and hydrogen-strontium forms

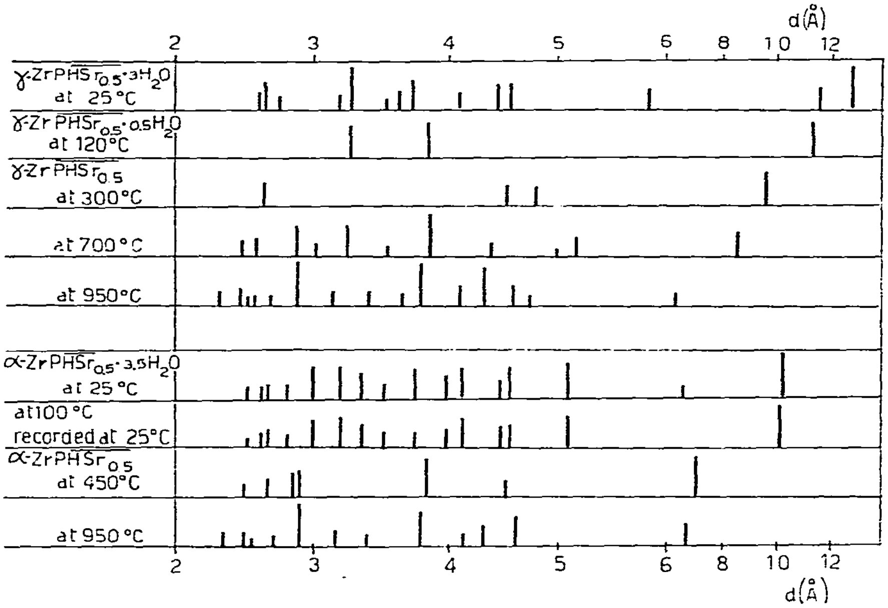

Fig. 11. X-Ray diffraction patterns of hydrogen-strontium forms of γ- and α-zirconium phosphates and their derivatives at various temperatures.

of α- and γ-ZrP also leads to the conclusion that products having the same chemical composition do not show any similarity, except at high temperatures when similar $ZrP_2O_7$, or sodium–, or strontium–zirconium phosphates or pyrophosphate are obtained.

## CONCLUSIONS

The results obtained by studying the thermal behaviour of the γ-phases of titanium and zirconium phosphates containing different exchangeable cations, such as H, Na or Sr, allow us to conclude that they generally behave differently from the corresponding α-phases. Even when α- and γ-forms have the same chemical composition (hydrated or anhydrous), their X-ray powder patterns are quite different and the γ-phases generally maintain a first *d*-value higher than that of the corresponding α-phases. This would indicate that marked differences in the structure of these two series of compounds exist initially and persist over a large temperature range. Only at high temperatures (800–900 °C) do the γ-compounds give pyrophosphate or double phosphate phases similar to those derived from the α-forms and the phase reaction is generally accompanied by an exothermal effect.

For as concerns the (as yet unknown) structure of the γ-compounds, the discontinuous decrease of their first *d*-value during the heating of hydrated or anhydrous phases, suggests that these materials also have a layered structure as observed for the α-forms.

The γ-TiP and γ-ZrP phases containing the same exchanged cation generally differ in their thermal behaviour, except for the hydrogen forms, for which some interesting similarities can be observed. Both γ-$TiP\overline{H_2}$ · $2H_2O$ (11.6 Å) and γ-$ZrP\overline{H_2}$ ·

$2H_2O$ (12.2 Å) reversibly lose their hydration water in two steps and show a parallel discontinuous change of the interlayer distance as the dehydration progresses with increase in the temperature (see Tables 1 and 2). In both cases, the condensation of the hydrogen phosphate groups proceeds through the formation of intermediate partially condensed phases, simulating a two-step process and finally the respective pyrophosphate phases transform, at high temperature (800–900 °C), into the already known α-pyrophosphates.

As observed for the α-forms[1,2], the dehydration process occurs at a lower temperature for $\gamma\text{-ZrP}\overline{\text{H}}_2 \cdot 2H_2O$ than for $\gamma\text{-TiP}\overline{\text{H}}_2 \cdot 2H_2O$. This is connected to several factors, one of which could be the higher electronegativity of titanium which probably involves a lower covalency in the $\gtrdot O_3P{-}OH$ groups; this, in turn, could lead to stronger bonds with the hydration water. The only difference in the parallel thermal behaviour of $\gamma\text{-TiP}\overline{\text{H}}_2 \cdot 2H_2O$ and $\gamma\text{-ZrP}\overline{\text{H}}_2 \cdot 2H_2O$ should be the reversible endothermic phase transition observed only for $\gamma\text{-ZrP}\overline{\text{H}}_2 \cdot 2H_2O$. However, from the X-ray powder patterns of this material taken before and after the thermal effect, it results that no marked structural modifications should take place when the phase transition occurs.

## REFERENCES

1 A. La Ginestra, M. A. Massucci, C. Ferragina and N. Tomassini, *Atti IX Conv. Naz. Chim. Inorg., Marina del Cantone, Assoc. Ital. Chim. Inorg., Padova, September 1976*, A4.
2 S. Allulli, C. Ferragina, A. La Ginestra, M. A. Massucci and N. Tomassini, *J. Inorg. Nucl. Chem.*, 39 (1977) 1043.
3 A. Clearfield, R. H. Blessing and J. A. Stynes, *J. Inorg. Nucl. Chem.*, 30 (1968) 2249.
4 G. Alberti, U. Costantino and M. L. Luciani-Giovagnotti, *J. Inorg. Nucl. Chem.*, submitted for publication.
5 G. Alberti, *Acc. Chem. Res.*, 11 (1978) 163.
6 A. Clearfield, G. H. Nancollas and R. H. Blessing, in J. A. Marinsky and Y. Marcus (Eds.), *Ion Exchange and Solvent Extraction*, Vol. 5, Marcel Dekker, New York, 1973.
7 G. Alberti, P. Cardini-Galli, U. Costantino and E. Torracca, *J. Inorg. Nucl. Chem.*, 29 (1967) 571.
8 G. Levi and G. Peyronel, *Z. Kristallogr.*, 92 (1935) 190.
9 S. Allulli, C. Ferragina, A. La Ginestra, M. A. Massucci, N. Tomassini and A. A. G. Tomlinson, *J. Chem. Soc., Dalton Trans.*, (1976) 2115.
10 C. Bettinali, A. La Ginestra and M. Valigi, *Atti Accad. Naz. Lincei, Sez. VIII*, 33 (1962) 472.
11 D. Dollimore, S. E. Horsley, N. J. Manning and D. V. Nowell, *Proc. 4th ICTA, Budapest, 1974*, Akad. Kiadó, Budapest, 1975, Vol. 1, p. 647.
12 A. La Ginestra, M. A. Massucci, C. Ferragina and N. Tomassini, *Proc. 4th ICTA, Budapest, 1974*, Akad. Kiadó, Budapest, 1975, Vol. 1, p. 631.
13 D. E. Harrison, H. A. McKinstry and F. A. Hummerl, *J. Am. Ceram. Soc.*, 37 (1954) 277.
14 A. Clearfield and A. S. Medina, *J. Inorg. Nucl. Chem.*, 32 (1970) 2775.
15 L. Hagman and P. Kierkegaard, *Acta Chem. Scand.*, 22 (1968) 1822.